

Osseointegration and Mechanical Stability of Pyrocarbon and Titanium Hand Implants in a Load-Bearing *In Vivo* Model for Small Joint Arthroplasty

Wolfgang Daecke, MD, Katrin Veyel, Peter Wieloch, MD,
Martin Jung, MD, Helga Lorenz, DVM, Abdul-Kader Martini, PhD, MD

From the Department of Orthopaedic Surgery, University of Heidelberg, Heidelberg, Germany.

Purpose: To test the mechanical stability and histologic osseointegration under load-bearing conditions of 2 different materials, pyrocarbon (Py) and titanium (Ti), in a rabbit model.

Methods: Proximal interphalangeal implants (9 Ti, 8 Py) were placed into rabbit knees and the animals were killed after 3 months. Subsidence was assessed by monthly x-rays. Mechanical stability was measured with a nondestructive pullout test. Implant osseointegration was evaluated by an analysis of the relative implant–calcified bone contact surface on microradiographs and by a histomorphometric analysis of the percentage of bone and connective tissue contact with the implant surface. Histologic examination included assessment of bone apposition on the basis of fluorochromes.

Results: Subsidence was found in all 8 Py implants but in none of the Ti group. All 9 Ti implants were mechanically stable; all 8 Py implants were loose. A significantly higher implant–bone contact was found for the Ti group compared with the Py group. Bone apposition increased with time and was highest for the Ti implants 6 weeks after implantation.

Conclusions: In the rabbit model osseointegration of implants was highly dependent on the material. A reliable osseointegration was found for Ti implants. For Py implants no osseointegration or implant stability was achieved. For use of small joints of the hand we therefore recommend Ti-based implants. (*J Hand Surg* 2006;31A:90–97. Copyright © 2006 by the American Society for Surgery of the Hand.)

Key words: Osseointegration, arthroplasty, hand, finger, PIP joint, animal model.

Implant arthroplasty in hand surgery remains a challenge and many problems relating to it have yet to be resolved. At present implants are available for the wrist, the distal ulnar head, the trapezometacarpal joint of the thumb, and the finger joints. Recently designed resurfacing hemiprostheses for the proximal scaphoid and the capitate have been introduced and may gain importance in the near future.^{1–4}

The cementless resurfacing implant arthroplasties currently available for hand surgery are manufactured using titanium (Ti) or pyrocarbon (Py).^{5–7} For Py, a material with good wear characteristics in articulation with cartilage, little is known about its osseointegration in a load-bearing model.⁸ Therefore the osseointegration and secondary implant stability of this material under loaded conditions is of major

interest. Because Ti can be considered a standard in cementless implant fixation for various joints, comparing the osseointegration of Py with that of Ti is a logical attempt to address this question.

A major problem in hand surgery is the lack of adequate and practical animal models in which a small prosthesis can be implanted, the joint of which would be comparable with the force in relation to implant size. Moreover the design of the implant must be adapted to the force distribution and anatomic structures. Because osseointegration is influenced by the primary implant stability and the micromovements of the implant under load, an adequate test setting should be performed under load-bearing conditions including shear forces. The rabbit knee model for testing finger implants, which first

was described by Minamikawa et al⁹ in 1994, enables implant assessment under load-bearing conditions.

The aim of this study was to test the mechanical stability and histologic osseointegration of Py and Ti in the load-bearing rabbit model.

Materials and Methods

Implants

Two different hemiprotheses were used in this study. The Ti implant (n = 10) (size 3; Avanta, San Diego, CA) consisted of a Ti-6Al-4V alloy stem with a pure Ti-sintered coating and a Co-Cr-Mo alloy-articulating surface at the cap. The Py implant (n = 10) (size 30P; Aescension, Austin, TX) consisted of a graphite core on which a layer of low-temperature isotropic pyrolytic carbon of approximately 0.5 mm in thickness was deposited. The designs of the Py and Ti implants were identical, with an angulation in the undercap surface and a cone-shaped, 4-square stem. The stem of each implant exceeded the press-fit anchorage zone of the 5-mm subcondylar cancellous bone stock. Because of the wide intramedullary cavity in rabbits no primary intramedullary stem–bone contact was possible.

Surgical Procedures

The 2 different hemiprotheses (proximal component) were placed into the right distal femur of mature New Zealand white rabbits (Charles River, Kisslegg, Germany). The animal experiment was approved by the Institutional Animal Care and Use Committee (Regierungspräsidium Baden-Württemberg, Karlsruhe, Germany; reference number AZ:35-9185.81/G-47/03). Based on preclinical tests on 30 rabbit knees the surgical approach, preservation of ligaments, preparation of the implant bearing, and positioning and design of the implants were standardized. The feasibility of the rabbit model was established on a further 5 animals with a testing period of up to 12 months.

The study was performed on 20 mature New Zealand white rabbits (age, 6 mo). Before surgery, diazepam (Valium; Fa. Roche, Basel, Switzerland) (2.5 mg/kg body weight) and atropinsulfate (B. Braun, Melsungen, Germany) (0.1 mg/kg body weight) were administered by intramuscular injection. General anesthesia was given by intravenous administration of ketamine (Ketavet; Pharmacia and Upjohn, Erlangen, Germany) (50 mg/kg body weight) and intramuscular injection of xylazine hydrochloride (Rompun 2%; BayerVital, Leverkusen, Germany) (5 mg/kg body weight). All surgeries were performed under sterile conditions in an animal op-

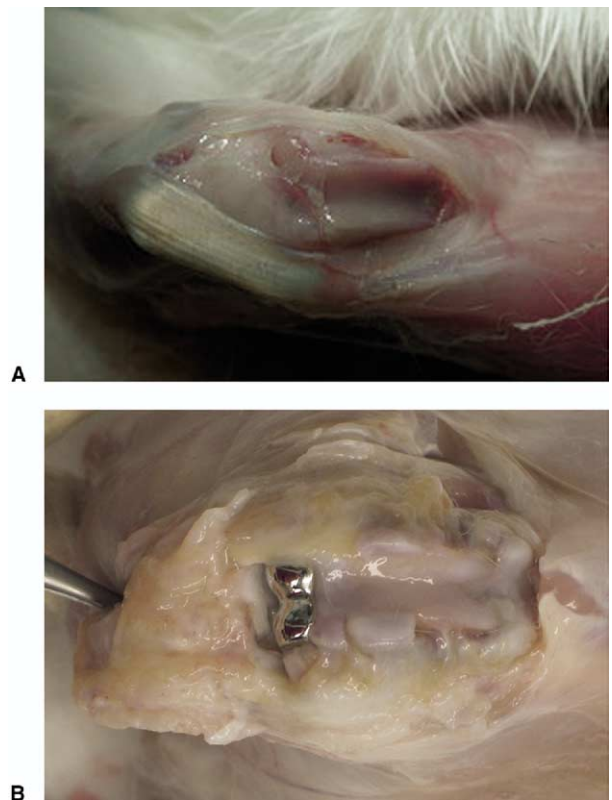


Figure 1. Surgical approach: (A) The patella was displaced laterally and the distal part of both femur condyles was resected. (B) Implant in place 3 months after implantation with the quadriceps tendon dissected proximally and the patella displaced distally.

erating theater. A medial arthrotomy was performed through a dorsal skin incision and the patella was displaced laterally (Fig. 1A). The distal part of both femoral condyles was resected with a 5-mm osteotome according to the shape of the undercup of the implant (Fig. 1B). Care was taken to preserve collateral ligaments and the posterior cruciate ligament. The anterior cruciate ligament had to be cut to open the medullary cavity. The preparation of the medullary cavity was performed by using ordinary undersized rasps. Both prostheses models were press-fit without cement. To achieve an optimal range of motion (ROM) in the rabbit knee and to decrease shear forces on the prosthesis the orientation of the implant was in a flexed position of 30° relative to the femur shaft. Before placement of the third prosthesis tantalum seeds (tantalum markers; Tilly, Lund, Sweden) were inserted into the distal femur as markers for radiologic analysis of implant migration. After insertion of the implant the stability and ROM of the knee were ascertained and closure of the capsule and skin was performed in separate layers with single resorbable sutures (Vicryl 3-0; Ethicon, Norderstedt, Germany). An analgesic was injected intramuscularly every 24 hours for 5 days (Temgesic, buprenor-

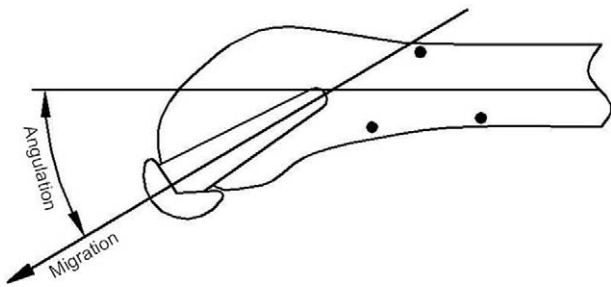


Figure 2. The subsidence of the implant was measured in reference to the tanatalum markers. Migration was defined as displacement along the axis of the implant and angulation as the tilt of the implant axis in relation to the femoral axis.

phine; Boehringer, Mannheim, Germany) (0.05 mg/kg body weight). Immediately after surgery the involved leg was splinted for 5 days in a custom-made splint in 90° of knee flexion. The first x-ray was obtained after splint removal. In a rabbit model a mature osseous response develops within 12 weeks after surgery.¹⁰ This period therefore was selected for the present *in vivo* study. The rabbits were kept in standard boxes (64 × 64 × 60 cm) for 6 weeks. For the remaining 6 weeks of the implantation period the rabbits were kept in large boxes (250 × 80 × 220 cm) to allow full weight-bearing under appropriate mobility. In cases of joint immobility, obvious implant failure on x-ray, or general impairment the animals were killed before the end of the study and excluded from further analysis.

After the animal were killed with an overdose of pentobarbital (Narcoren; Merial, Hallbergmoos, Germany) the right femurs were explanted.

Range of Motion and Clinical Gait Analysis

At the end of the follow-up period, the passive ROMs of the involved knees were measured.

Gait analysis of each subject was classified according to 2 categories: (1) normal gait: complete load, no lameness and (2) impaired gait: reduced weight-bearing, lameness. Classifications were assessed by 2 observers.

Radiologic Examination

X-rays of the involved knees were taken (with sedation) in 2 planes 5 days after surgery, at a 1- and 2-month interval, and after killing the animals 3 months after surgery. Based on a radiographic series the subsidence (migration and angulation) was assessed (Fig. 2). Implant migration was measured by the difference in the distance from the implant to the intraosseous tanatalum markers. An x-ray-related magnification was excluded by controlling the length of the implant on each x-ray. Negative migration was defined as an implant migration in the tibial direc-

tion. Angulation of the implant was measured as the change of the implant axis in relation to the femoral axis when comparing the mediolateral x-rays. An angulation of the implant axis into extension in relation to the femur shaft was defined as positive. The occurrence of radiolucencies or sclerosis around the implant was evaluated for 3 different regions (cup, stem, tip) on all x-rays. Microradiographs were obtained from all implants and assessed for evidence of fracture, bony resorption, occurrence of radiolucent lines, and relative implant–calcified bone contact. The last was evaluated on digitized microradiographs (magnification, ×10) by an operator-assisted morphometry (Vision AxioVision LE Rel. 4.3; Carl Zeiss, Göttingen, Germany). Because of the non-radiodense outer Py layer of the Py implants a layer of 0.5 mm was added to the visible implant border.

Mechanical Stability

After retrieval of the femur the stability of the implant first was tested by manual pulling (2-finger pinch of approximately 0.5 kg/m²; pulling force to implant, 0.5 N). Only those implants that were affixed firmly to the bone were evaluated further by a pullout test. For mechanical testing of the bone–implant interface a nondestructive pullout test was adapted for the study. A pull plate and preload were connected perpendicular to the implant by a clamp mechanism. Three 1- μ m length sensors (LVDT#1300; Fa. Mahr, Göttingen, Germany) were adjusted at defined positions on the plate to determine displacement of the implant along its long axis in relation to a fourth sensor positioned on the femur. The system was calibrated and the pull plate was loaded to 3 kg and then unloaded gradually. During loading and unloading the maximum elastic displacement of the implant relative to its bone stock was recorded with a computer program designed specifically for this purpose.¹¹ Because of the 3-point configuration of the length sensors the tilt of the pull plate was adjusted by calculating the sum vector with a computer program (AutoCAD, Mechanical Desktop; Autodesk Inc., San Rafael, CA). The amount of calculated displacement is known to be related to the thickness of the interface layer and the amount of osseointegration.¹² An elastic micromovement of less than 100 μ m was rated as a stable implant–bone interface.¹² If the end position had changed more than 20% relative to the start position a plastic deformation was assumed and the specimen was rated as mobile.

Histologic Examination

In all animals fluorochromes were injected subcutaneously according to the following protocol: calcein green (30 mg/kg body weight) was administered on the 7th day, xylene orange (90 mg/kg body weight)

on the 21st day, and oxytetracyclin (15 mg/kg body weight) on the 42nd day. After mechanical testing within 6 hours after killing the animals the femur specimens were fixed in formalin solution for 3 days and dehydrated in a graded series of ethanol. The retrieved femurs were embedded in methyl methacrylate (Technivit9100; Heraeus Kulzer, Dormagen, Germany). Nondecalcified serial longitudinal sections were cut using a water-cooled diamond saw (Exakt-Apparatebau, Norderstedt, Germany). The longitudinal sections along the midportion of the implant were mounted on Plexiglas slides (Cadillac Plastik, Viernheim, Germany), then ground and polished on a precision grinder (Exakt-Apparatebau) to a thickness of 100 to 150 μm .

Operator-assisted histomorphometry (Vision AxioVision Rel. 4.3; Carl Zeiss) was used for blinded quantification of the tissue response around the implant. With an unstained specimen under epifluorescent light at a magnification of 25 times, the new bone area (bone apposition) within a circumferential zone of 500 μm around the implant was measured and the percentage of new bone was calculated for each level. Filters of wavelengths 510 to 560 nm (green filter), 450 to 490 nm (blue filter), and 340 to 380 nm (ultraviolet filter) (Carl Zeiss) were used.¹³⁻¹⁵ For histomorphometric analysis trichome Masson-Goldner staining was performed. The images were assessed at a magnification of 100 times and digitized (Vision AxioVision Rel. 4.3; Carl Zeiss). The length of the implant surface in contact with bone and connective tissue and without tissue contact (gap) was measured for the whole implant (overall) and at defined zones for the cup, stem, and tip of the implant on Masson-Goldner-stained specimens. The corresponding implant circumference was measured to allow calculation of the percentage of bone and connective tissue contact and with implant surface or the surrounding gap.¹⁰ Additionally an inflammatory score (more than 10 polymorphonuclear leukocytes in 1 high-power field, more than 10,000 cells/mL in the aspiration, and radiologic signs of a lytic defect) was applied to identify implant loosening caused by infection.¹⁶ To eliminate a variation in estimates by different investigators the same blinded investigator performed all histomorphometric analyses.

Exclusion Criteria

All animals that had to be killed for any reason before the end of study were excluded from the analysis. Implant fracture, implant dislocation, and a positive inflammatory score were additional exclusion criteria.

Statistics

The mean and SD were calculated for all continuous parameters. The association between 2 continuous variables of different groups was tested by the unpaired Student *t* test. The paired *t* test was applied to compare intragroup continuous parameters, and the Pearson chi-square test was used for comparison of discrete variables. A 2-tailed *p* value equal to or less than .05 was considered significant. All tests were without α adjustment. Data analysis was performed with statistical software (SPSS for Windows 11.0.1; SPSS Inc, Chicago, IL).¹⁷

Results

After surgery all animals recovered well; however, their mean weight decreased significantly throughout the follow-up period (before surgery, 4.0 ± 0.5 kg; at termination, 3.4 ± 0.4 kg; $p = .001$). Animal weight did not differ significantly between the 2 implant groups. No problem with soft-tissue healing was observed.

Exclusion of Animals From the Study

Three of the 20 animals were excluded from analysis. One animal from the Ti group was excluded because of histologic evidence of chronic implant infection. Microradiographs showed periprosthetic radiolucencies in the distal femur. The migration of this implant was 0.3 mm and the angulation was 10° within 3 months. On manual testing this Ti implant was mobile.

In the Py group 2 specimens were excluded because of 1 implant fracture and 1 implant dislocation. The gait of the 2 animals was classified as impaired.

Range of Motion and Clinical Gait Analysis

The average range of motion immediately after surgery was $127^\circ \pm 9^\circ$ for the Ti group ($n = 9$) and $126^\circ \pm 10^\circ$ for the Py group ($n = 8$). After the follow-up period the ROM was $99^\circ \pm 19^\circ$ for the Ti group and $104^\circ \pm 25^\circ$ for the Py group. With time the ROM in the Ti group decreased significantly ($p = .009$). The Py group showed a trend toward decreased ROM ($p = .065$). Differences in ROMs between the groups were insignificant.

On clinical gait analysis before termination all 9 animals from the Ti group and 8 animals from the Py group were classified as normal.

Radiographic Results

By analysis of serial radiographs of Ti implants no angulation (0°) was found in the 9 animals. One of those 9 implants showed a migration of 0.6 mm only in the first month. X-rays showed no radiolucencies in any implant region. Periprosthetic sclerosis in-

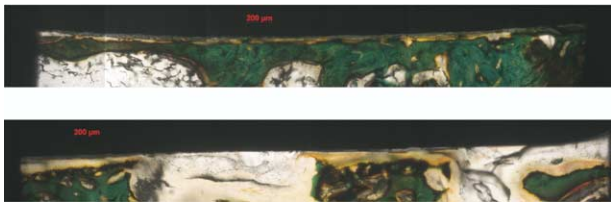


Figure 3. Bone tissue contact area of (A) Ti and (B) Py stem (magnification, $\times 100$). On the basis of the Masson-Goldner staining uncalcified bone (osteoid) is red, calcified bone is green, and connective tissue is stained in brown. Note the direct implant–bone contact zone at the Ti implant.

creased with time and was found in the beginning only at the cup but also occurred at the stem with time. On microradiographs the 9 Ti implants were well integrated with no evidence of fractures, bony resorption, or radiolucent line. The relative implant–calcified bone contact surface was $54.2\% \pm 24.1\%$.

Migration and angulation on serial radiographs were found in all 8 Py implants, with an average value of -0.5 ± 1.0 mm and $4.3^\circ \pm 3.6^\circ$, respectively, in the first month; -1.0 ± 0.8 mm and $7.1^\circ \pm 5.0^\circ$, respectively, at 2 months; and -1.5 ± 0.8 mm and $8.6^\circ \pm 6.3^\circ$ at 3 months. The difference in migration (except for the first month) and angulation of the Py implant compared with the Ti implant was significant ($p < .03$). Assessment of radiolucencies on serial radiographs was limited because of the nonradiodense outer Py layer. Periprosthetic sclerosis increased with time and was found in all regions of the implant at the end of the implant period. On microradiographs a radiolucent line extending beyond the nonradiodense layer was observed in all animals. No fracture occurred but bony resorption was obvious at the implant tip in 7 specimens. The relative implant–calcified bone contact surface was $23.3\% \pm 18.6\%$. The implant–calcified bone contact of Py implants was significantly lower than that of Ti implants ($p = .01$).

Mechanical Testing

On gentle manual pulling all 9 Ti implants were affixed firmly to the bone. In the nondestructive pullout test the average elastic microdisplacement of these 9 implants was 20 ± 9 μm . The mechanical implant stability of the Py group was nonexistent. In all 8 animals in the Py group the implants were mobile relative to the bone by the manual test. Therefore the nondestructive pullout test with a preload of 1.5 kg could not be applied.

Histologic Examination

The Ti group showed an overall significantly higher bone–implant contact and implant–connective tissue

contact compared with the Py group (Fig. 3). The overall implant gap was significantly lower for the Ti group compared with the Py group. Of the 2 materials Py showed the highest percentage of implant surrounding the gap, especially at the tip of the implant. Implant–tissue contacts for the different implant regions (cup, stem, tip) are shown in Table 1. The overall bone apposition within the circumferential zone was significantly higher for the Ti group compared with the Py group 6 weeks after implantation ($p = .015$) (Fig. 4). Six weeks after implantation the bone apposition of the Ti group was higher at the cup (2.8%) and the stem (2.4%) than at the tip (1.6%) of the implant (Fig. 5A). The bone formation of the Py group at 6 weeks after surgery was mostly at the tip of the implant (2.3%) and was lower at the cup (0.7%) and stem (1.5%) (Fig. 5B).

Discussion

The aim of this study was to test the osseointegration and secondary implant stability under load-bearing conditions of 2 different materials used in hand arthroplasty by using a rabbit model. It is well known that the force distribution of the rabbit knee is altered and generally higher compared with the finger joints. The loading force of the rabbit knee has been estimated to be up to 4 times the body weight, at approximately 100 N, whereas in the human proximal interphalangeal (PIP) joint the force is expected to be in the range of 25 N.^{18,19} In contrast to the finger joint the extension force in relation to the flexion force is higher in the rabbit knee. Furthermore anatomic structures vary—that is, there are no cruciate ligaments and meniscuses in finger joints. Because of a wider medullary cavity the primary implant–bone contact area is smaller in the rabbit femur than in the proximal phalanx of a human finger, which is only in the trabecular bone stock of the undercup area. The axis of joint movement is comparable, however, and in this study the overall ROM exceeded the ROM of a human PIP joint by 20% only directly after implantation. At the end of the study the average ROM was the same as in human finger joints.

In this animal model the proximal component of resurfacing PIP implants fits into the distal femur and preservation of joint stability and function can be achieved. Most important, this model allows for analysis of osseointegration of the different materials under *in vivo* conditions, and the conditions for each type of implant are thus the same. In addition this *in vivo* test for PIP implants is performed under load-bearing conditions, the importance of which were shown by Soballe,¹² who reported that bone formation is modulated in a load-bearing situation. Similar to the finger joint, in the rabbit knee model synovial

Table 1. Implant–Bone Contact, Implant–Connective Tissue Contact, and Implant–Gap for the Type of Implant Overall, and at the Cup, Stem, and Tip of Implant

Type and Region of Implant	Ti			Py			Ti Overall vs Py Overall (p)	
	Cup	Stem	Tip	Overall	Cup	Stem		Tip
Number of sections	18	18	18	16	16	16	16	
Implant–bone contact (%)	55.4 ± 16.6	42.1 ± 9.9	55.0 ± 32.0	49.4 ± 13.3	15.7 ± 20.6	21.7 ± 13.6	0.7 ± 1.8	15.1 ± 10.2
Implant–connective tissue contact (%)	34.9 ± 16.6	52.2 ± 5.9	45.0 ± 32.0	43.7 ± 10.5	27.4 ± 18.3	39.6 ± 30.9	5.4 ± 10.8	27.9 ± 16.4
Implant–gap (%)	9.7 ± 9.6	5.7 ± 9.9	0 ± 0	6.9 ± 7.3	57.0 ± 30.7	38.5.0 ± 32.3	93.9 ± 11.6	57.0 ± 18.8

The overall contact between the 2 groups was evaluated by the unpaired *t* test. The highest implant–bone contact rate was found for the Ti implant in any region.

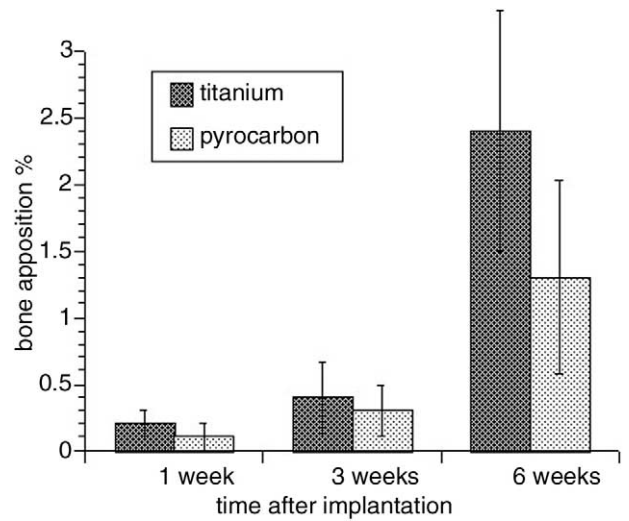


Figure 4. The overall bone apposition given as a percentage within a circumferential zone of 500 μm around the implant at 1 week, 3 weeks, and 6 weeks after implantation in relation to the type of implant.

fluid penetrates the bone–implant interface, probably interfering with the osseointegration.²⁰

In the present study significant differences in osseointegration in the 2 different prostheses were observed. As expected all 9 Ti implants—the gold standard in cementless implant materials—showed a solid osseointegration both mechanically and histologically. The only implant failure observed was related to infection. The reliable osseointegration of the standard material, Ti, confirms that the rabbit model is suitable for testing osseointegration under load-bearing conditions in different materials.

In contrast to Ti none of the Py arthroplasties presented a secure bony fixation. Implant subsidence was seen by serial radiograph analysis in every animal of the Py group. On mechanical testing by gentle manual manipulation all of the Py implants were found to be loose, which was why the nondestructive pullout test seemed pointless. Nondecalcified histologic evaluation of the Py implant showed various degrees of fibrous tissue enhancement and surrounding gap. As a result the implant–gap ratio was significantly higher for Py compared with Ti. The implant–bone contact proportion on histologic evaluation and the relative implant–calcified bone contact surface on microradiograph both were significantly lower for Py implants when compared with the Ti type.

Because of the increasing number of cementless implanted Py prostheses in humans our results are highly relevant. Previous publications^{21,22} on the osseointegration of Py in an unloaded model concluded that osseointegration of this material is possible. Thorough interpretation of the data of Anderson et al,²¹ however,

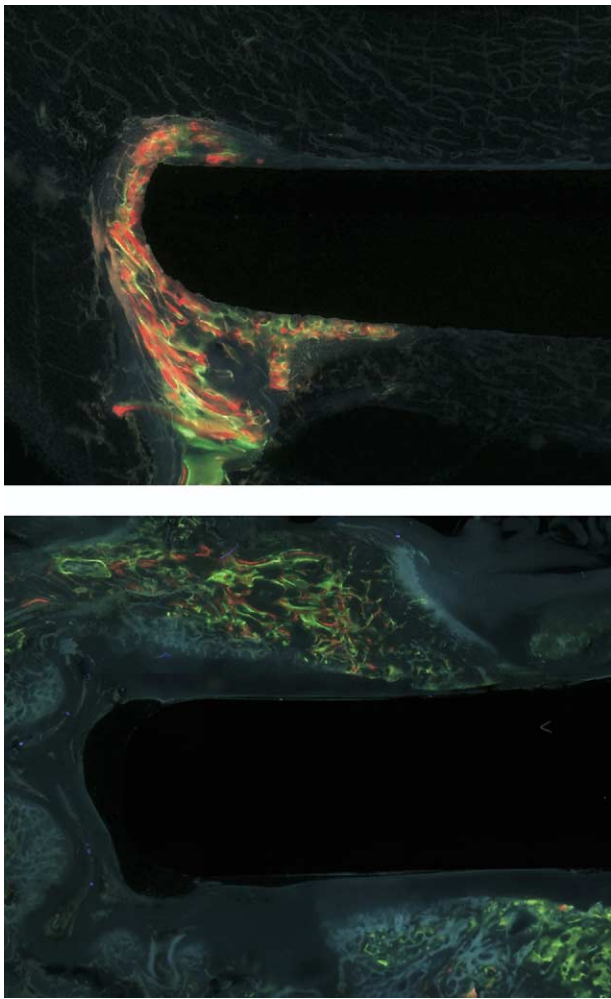


Figure 5. Unstained specimen of a (A) Ti (B) and Py implant tips under epifluorescent light (magnification, $\times 25$). The green-colored areas represent bone apposition after 1 week, the red areas after 3 weeks, and the yellow areas after 6 weeks.

show that the mechanical stability of this material evaluated by the load displacement curves was considerably lower, at approximately 150 N compared with 1,780 N for Ti. According to Hetherington et al,²³ “a non-bonded bone response to the carbon implants” was found and interpreted as a “lack of fixation” in a non-weight-bearing beagle model. Under load-bearing conditions a secure fixation of the Py implant cannot be achieved, at least in the rabbit knee model. The transfer of our findings to human conditions is limited; however, in a recent publication on short-term results of Py PIP implants an implant migration also was observed clinically.⁷ This conforms to the results of our animal model, underlining our findings of an insufficient osseointegration of Py.

The material itself has a high impact on the osseointegration and secondary stability for implants in the load-bearing rabbit model. For Py, a material increasingly used for cementless prostheses in the hand, no osseointegration and secondary stability

were achieved. Because Ti implants enable reliable osseointegration we recommend the use of Ti-based implants.

The authors thank Priv. Doz. Dr. I. Berger, PhD, MD (Department of Pathology, University of Heidelberg) for her support of the histologic analysis and Dr. Sven Schneider, DPhil MA (Division of Experimental Orthopaedics) for statistical support. For technical support the authors thank Dr. C. Lee, MD (Laboratory for Biomechanical and Implant Research, University of Heidelberg), Dipl. Ing. W. Roth, and G. Buchmann (Division of Experimental Orthopaedics).

Received for publication June 2, 2005; accepted in revised form October 4, 2005.

No benefits in any form have been received or will be received from a commercial party related directly or indirectly to the subject of this article.

Supported by a grant from the research fund of the Stiftung Orthopädische Universitätsklinik Heidelberg.

Corresponding author: Dr. Wolfgang Daecke, Orthopädische Universitätsklinik Heidelberg, Schlierbacher Landstraße 200a, 69118 Heidelberg, Germany; e-mail: wolfgang.daecke@ok.uni-heidelberg.de.

Copyright © 2006 by the American Society for Surgery of the Hand 0363-5023/06/31A01-0017\$32.00/0
doi:10.1016/j.jhsa.2005.10.002

References

1. Isselin J. Partial wrist prosthesis: concept and preliminary results in 13 cases. *Chir Main* 2003;22:144–147.
2. Pequignot JP, Lussiez B, Allieu Y. An adaptive proximal scaphoid implant. *Chir Main* 2000;19:276–285.
3. Costi J, Krishnan J, Percy M. Total wrist arthroplasty: a quantitative review of the last 30 years. *J Rheumatol* 1998; 25:451–458.
4. Linscheid RL. Implant arthroplasty of the hand: retrospective and prospective considerations. *J Hand Surg* 2000;25A: 796–816.
5. Sauerbier M, Cooney WP, Berger RA, Linscheid RL. Complete superficial replacement of the middle finger joint—long-term outcome and surgical technique. *Handchir Mikrochir Plast Chir* 2000;32:411–418.
6. Johnstone BR. Proximal interphalangeal joint surface replacement arthroplasty. *Hand Surg* 2001;6:1–11.
7. Schulz M, Muller-Zimmermann A, Behrend M, Krimmer H. Early results of proximal interphalangeal joint replacement with pyrolytic carbon prosthesis (Ascension) in idiopathic and post-traumatic arthritis. *Handchir Mikrochir Plast Chir* 2005;37:26–34.
8. Cook SD, Thomas KA, Kester MA. Wear characteristics of the canine acetabulum against different femoral prostheses. *J Bone Joint Surg* 1989;71B:189–197.
9. Minamikawa Y, Peimer CA, Ogawa R, Howard C, Sherwin FS. In vivo experimental analysis of silicone implants on bone and soft tissue. *J Hand Surg* 1994;19A:575–583.
10. Hacking SA, Tanzer M, Harvey EJ, Krygier JJ, Bobyn JD. Relative contributions of chemistry and topography to the osseointegration of hydroxyapatite coatings. *Clin Orthop Rel Res* 2002;24–38.
11. Gortz W, Nagerl UV, Nagerl H, Thomsen M. Spatial micro-movements of uncemented femoral components after torsional loads. *J Biomech Eng* 2002;124:706–713.
12. Soballe K. Hydroxyapatite ceramic coating for bone implant fixation. Mechanical and histological studies in dogs. *Acta Orthop Scand Suppl* 1993;255:1–58.
13. Nkenke E, Kloss F, Wiltfang J, Schultze-Mosgau S, Radespiel-Troger M, Loos K, Neukam FW. Histomorphometric and fluorescence microscopic analysis of bone remodelling

- after installation of implants using an osteotome technique. *Clin Oral Implant Res* 2002;13:595–602.
14. Matsumoto H, Ochi M, Abiko Y, Hirose Y, Kaku T, Sakaguchi K. Pulsed electromagnetic fields promote bone formation around dental implants inserted into the femur of rabbits. *Clin Oral Implant Res* 2000;11:354–360.
 15. Jinno T, Davy DT, Goldberg VM. Comparison of hydroxyapatite and hydroxyapatite tricalcium-phosphate coatings. *J Arthroplasty* 2002;17:902–909.
 16. Della Valle C, Zuckerman J, Di Cesare P. Periprosthetic sepsis. *Clin Orthop* 2004;420:26–31.
 17. Griffin D, Audige L. Common statistical methods in orthopaedic clinical studies. *Clin Orthop Rel Res* 2003;70–79.
 18. Fowler NK, Nicol AC. Measurement of external three-dimensional interphalangeal loads applied during activities of daily living. *Clin Biomech (Bristol, Avon)* 1999;14:646–652.
 19. Kaab MJ, Ito K, Clark JM, Notzli HP. Deformation of articular cartilage collagen structure under static and cyclic loading. *J Orthop Res* 1998;16:743–751.
 20. Schmalzried TP, Jasty M, Harris WH. Periprosthetic bone loss in total hip arthroplasty. Polyethylene wear debris and the concept of the effective joint space. *J Bone Joint Surg* 1992;74A:849–863.
 21. Anderson RC, Cook SD, Weinstein AM, Haddad RJ Jr. An evaluation of skeletal attachment to LTI pyrolytic carbon, porous titanium, and carbon-coated porous titanium implants. *Clin Orthop* 1984;182:242–257.
 22. Kevin TA, Cook SD. An evaluation of variables influencing implant fixation by direct bone apposition. *J Bio Med Mater Res* 1985;19:875–901.
 23. Hetherington VJ, Lord CE, Brown SA. Mechanical and histological fixation of hydroxylapatite-coated pyrolytic carbon and titanium alloy implants: a report of short-term results. *J Appl Biomater* 1995;6:243–248.